Anomalous Landau Level Gaps Near Magnetic Transitions in Monolayer WSe_2

Benjamin A. Foutty,[1,2] Vladimir Calvera,[2] Zhaoyu Han,[2] Carlos R. Kometter,[1,2] Song Liu,[3] Kenji Watanabe,[4] Takashi Taniguchi,[5] James C. Hone,[3] Steven A. Kivelson,[2] and Benjamin E. Feldman[1,2,6,*]

[1] *Geballe Laboratory for Advanced Materials, Stanford, California 94305, USA*
[2] *Department of Physics, Stanford University, Stanford, California 94305, USA*
[3] *Department of Mechanical Engineering, Columbia University, New York, New York 10027, USA*
[4] *Research Center for Electronic and Optical Materials, National Institute for Materials Science, 1-1 Namiki, Tsukuba 305-0044, Japan*
[5] *Research Center for Materials Nanoarchitectonics, National Institute for Materials Science, 1-1 Namiki, Tsukuba 305-0044, Japan*
[6] *Stanford Institute for Materials and Energy Sciences, SLAC National Accelerator Laboratory, Menlo Park, California 94025, USA*

(Received 14 February 2024; revised 21 June 2024; accepted 25 June 2024; published 1 August 2024)

First-order phase transitions produce abrupt changes to the character of both ground and excited electronic states. Here we conduct electronic compressibility measurements to map the spin phase diagram and Landau level (LL) energies of monolayer WSe_2 in a magnetic field. We resolve a sequence of first-order phase transitions between completely spin-polarized LLs and states with LLs of both spins. Unexpectedly, the LL gaps are roughly constant over a wide range of magnetic fields below the transitions, which we show reflects spin-polarized ground states with opposite spin excitations. These transitions also extend into compressible regimes, with a sawtooth boundary between full and partial spin polarization. We link these observations to the important influence of LL filling on the exchange energy beyond a smooth density-dependent contribution. Our results show that WSe_2 realizes a unique hierarchy of energy scales where such effects induce reentrant magnetic phase transitions tuned by density and magnetic field.

DOI: 10.1103/PhysRevX.14.031018 Subject Areas: Condensed Matter Physics

I. INTRODUCTION

Electronic systems with degeneracies arising from internal quantum degrees of freedom are often susceptible to forming ordered ground states driven by many-body interactions. The quantum Hall regime, in which Landau levels (LLs) effectively quench kinetic energy, provides a model platform to study such phases and the transitions between them. In particular, the relative energies of LLs with distinct spin and/or valley indices can often be modified by experimental tuning knobs which affect both the many-body ground and excited states in these systems [1–16]. However, the nature of charge excitations near transitions between competitive LLs depends sensitively on details of the LL energetics and can be difficult to directly probe.

Monolayer semiconducting transition metal dichalcogenides realize a distinctive LL structure due to their hierarchy of energy scales. Strong spin-orbit coupling near the valence band maxima at valleys K and K' causes the relevant low-energy bands to be spin-valley locked, so that only a single Ising spin orientation is relevant at each valley [17]. This degree of freedom forms a generalized isospin, which we refer to as spin in the rest of the text. A combination of the large effective mass and the additive contributions of orbital and Berry-curvature effects produces a single-particle Zeeman splitting of the valence band E_Z^0 that is large relative to the cyclotron energy E_{cyc} in monolayer WSe_2 ($E_Z^0/E_{\mathrm{cyc}} \approx 2$) [18]. The large effective mass also enhances the relative importance of interactions, such that the dimensionless parameter r_s is of the order of 5–10 at achievable carrier densities [19].

Prior work has shown that these interactions drive a density-dependent exchange enhancement of the effective Zeeman energy E_Z [9,18,20]. This increases the spin splitting of the valence bands as the hole density decreases and leads to preferential occupation of fully spin-polarized LLs at low densities [Fig. 1(a)] [19]. At higher densities, both "majority" and "minority" spin Zeeman-split LLs are occupied, causing alternating LL gap sizes dominated by even or odd integers [9,18,20–22]. Recent studies have noted the possibility of first-order phase transitions at the crossover between these limits in monolayer WSe_2 and

*Contact author: bef@stanford.edu

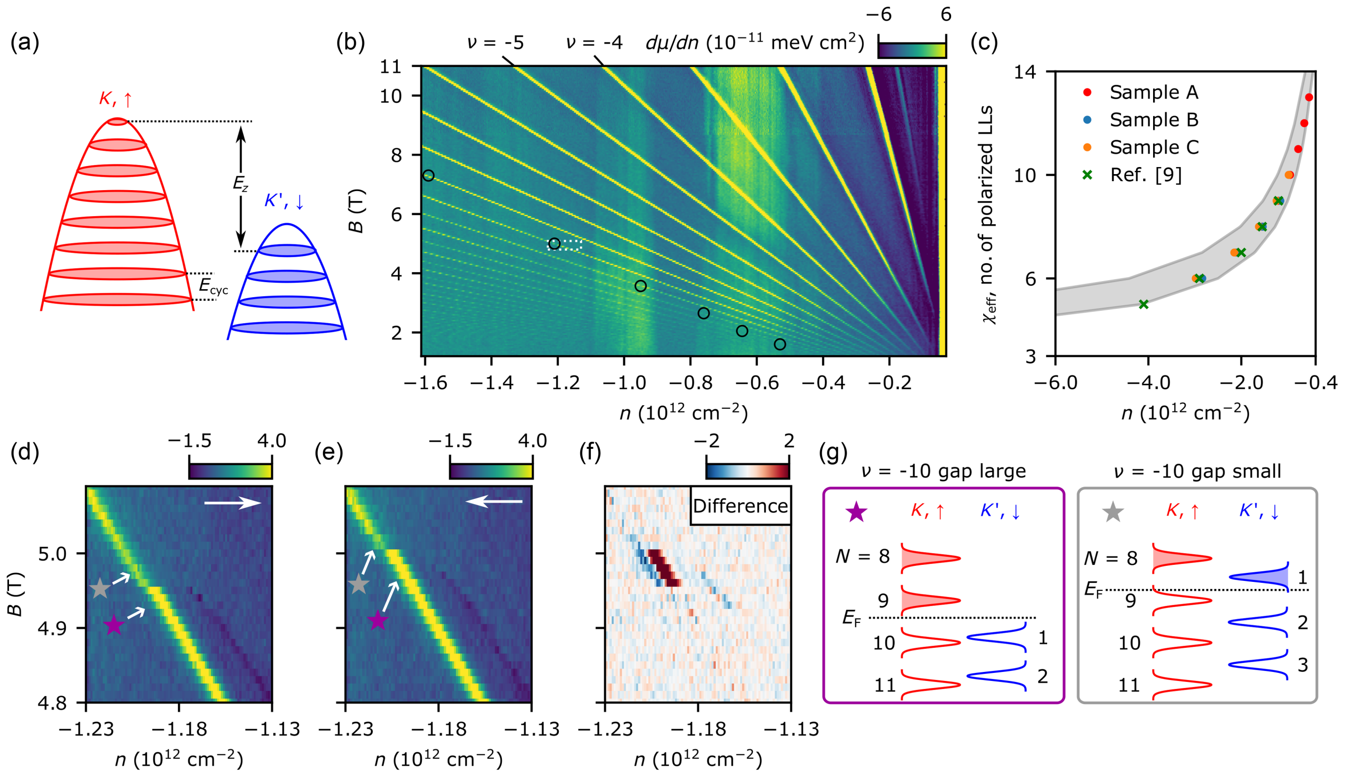

FIG. 1. First-order Landau level (LL) phase transitions in monolayer WSe_2. (a) Schematic of the valence band LL structure in monolayer WSe_2. The two relevant bands are spin up at valley K and spin down at valley K', which are split by a density-dependent effective Zeeman energy E_Z. E_{cyc} is the cyclotron energy. (b) Inverse electronic compressibility $d\mu/dn$ in monolayer WSe_2 as a function of hole density n and perpendicular magnetic field B. Black circles mark sharp drops in the magnitude of $d\mu/dn$ along incompressible LL gaps. Broad vertical features are artifacts due to long ac charging time of the sample (Supplemental Material Sec. I [25]). (c) Spin susceptibility χ_{eff} as a function of n, determined from the densities of the LL transitions [such as those highlighted in (b)] from three distinct samples. We also present data from Ref. [9] and theoretical predictions based on quantum Monte Carlo calculations shaded in gray for comparison. (d),(e) Enlargements of $d\mu/dn$ in the white box in (b), with the density swept in opposite directions (large white arrows). (f) Difference between (d) and (e), demonstrating pronounced hysteresis from a first-order phase transition. (g) Schematics of LL energies that respectively correspond to the starred positions in (d) and (e); note that due to the hole carriers, states are filled from the top downward. N denotes the LL orbital index and E_F is the Fermi level.

related systems, but hysteresis has not been observed and a detailed understanding of the LL energetics as the system transitions from fully to partially spin polarized has until now been lacking [9,23,24].

In this work, we use a scanning single-electron transistor to measure the inverse electronic compressibility $d\mu/dn$ of valence band holes in monolayer WSe_2 in a perpendicular magnetic field. At the crossover between fully spin-polarized LLs and the lowest-energy minority spin LL being filled, we resolve first-order phase transitions, including hysteresis in the LL gaps and adjoining sharp tails of negative compressibility that extend outward into nearby compressible electronic states. Surprisingly, the LL gaps are roughly constant over a wide range of magnetic fields below these phase transitions. Through high-resolution measurements of the thermodynamic LL gaps and the first-order phase transitions, together with supporting theoretical calculations, we systematically characterize the nature of low-energy charge excitations throughout the phase diagram. Collectively, these indicate multiple reorderings of the LL structure as we vary carrier density and magnetic field. Our results provide a straightforward way, in the correlation-dominated regime, to understand the spin character and energies of ground and excited electronic states.

II. FIRST-ORDER SPIN TRANSITIONS

In Fig. 1(b), we present a Landau fan of $d\mu/dn$ as a function of carrier density n and perpendicular magnetic field B. Across data from three distinct devices, we observe qualitatively similar behavior, though we focus on data from a single sample through most of the main text (see Supplemental Material Sec. II for a detailed comparison [25]). Most of the incompressible features can be identified via their slope in the n-B plane as integer quantum Hall gaps, which occur at all integer filling factors ν. Additionally, we note fractional quantum Hall states in the lowest LL consistent with previous reports [9,26] (Supplemental Material Sec. III [25]).

Following constant integer ν, we observe abrupt drops in the magnitude of the LL gaps [marked by black circles in Fig. 1(b)] that occur when the first minority spin LL crosses the highest occupied majority spin LL, corresponding to a transition from full to partial spin polarization [9]. We determine the effective spin susceptibility χ_{eff} by identifying the number of polarized LLs at the phase transitions [9,10,27]. Note that this is actually a response to a finite field, and can strictly be identified as the "susceptibility" in the noninteracting limit. We find that χ_{eff} extends up to 13, corresponding to a g factor of roughly 35 at the lowest density transition that we can resolve [Fig. 1(c)]. The observed increase of χ_{eff} with decreasing hole density is broadly consistent with previous quantum Monte Carlo calculations of a 2D electron gas, shaded in gray [27,28] (Supplemental Material Sec. IX [25]).

We resolve hysteresis in both the LL gaps and adjacent negative compressibility features (discussed in detail below) as shown in Figs. 1(d)–1(f), direct evidence of first-order phase transitions. As the hole density is swept in opposite directions, the sharp drop in gap size occurs at distinct magnetic fields (we also observe signatures of hysteresis upon sweeping B; see Supplemental Material Sec. II [25]). The behavior reflects spontaneous polarization switching of the last occupied LL [Fig. 1(g)] [23,24]. Specifically, the large gap is stabilized when sweeping from a fully polarized phase, where exchange interactions favor maintaining maximum spin polarization and enhance the effective g factor [29]. We only resolve hysteresis as the first (orbital index $N = 1$) minority spin LL becomes competitive with the valence majority spin level; at lower magnetic fields at the same density where LLs with higher indices cross, there are no sharp changes in the measured gaps (Supplemental Material Sec. IV [25]). This indicates that the additional g-factor enhancement is suppressed when both majority and minority spin LLs are occupied, destroying the expected first-order transition or rendering it undetectably weak.

III. ANOMALOUS LL GAP SCALING

Our measurements encode information not only about changes in the occupied LLs, but also about excited states immediately above the Fermi level. To study the LL energetics in the vicinity of the spin phase transitions, we integrate $d\mu/dn$ to obtain the thermodynamic gaps Δ_ν at integer filling factors ν (Fig. 2). For each integer quantum Hall gap, we observe three distinct behaviors as a function of magnetic field. We relate these behaviors to distinct ground states and their lowest-energy charge excitations, as detailed below.

At fixed filling factor and low fields, highlighted by a red "P" in Figs. 2(a)–2(e), the LLs are fully spin polarized. We observe a linear field dependence of these gaps, indicating that they are set by the cyclotron energy $E_{\mathrm{cyc}} = (\hbar eB/m^*)$ to the next spin-majority LL. We extract an effective mass $m^* \approx 0.31 m_e$ from the linear slope, where $\hbar$ is the reduced Planck's constant and e and m_e are the electron charge and mass (m^* depends weakly on sample; see Supplemental Material Sec. II [25]). At fixed filling factor and sufficiently high field, highlighted by a gray "M" in Fig. 2, the LLs are in a "mixed" regime where both spins are occupied. Individual gaps grow and shrink as the density-dependent effective Zeeman energy changes the relative spacing between LLs of different spin, but the pairwise sum of gaps $\Delta_\nu + \Delta_{\nu+1}$ at a given density matches the cyclotron energy with a similar effective mass to that of the polarized LLs [Fig. 2(k); see Supplemental Material Sec. V [25]]. This is in agreement with prior measurements of LL gap sizes in monolayer WSe_2 at higher hole densities, though we measure a slightly lower effective mass [18] (Supplemental Material Sec. II [25]). Both the polarized and mixed regimes can be well described by the previously considered model in which LLs are affected by a smooth density-dependent Zeeman enhancement but are otherwise unchanged energetically [9]. Our experiments, however, demonstrate a more complicated behavior at the transition between these regions.

Between the polarized and mixed regimes, we observe that each LL gap plateaus as the field is increased preceding its first-order phase transition. Remarkably, the range of magnetic fields over which the gaps are flat, highlighted by a purple "T" in Fig. 2, can extend over several Tesla (e.g., between 6.5 and 11 T for $\nu = -8$). At a given density, two gaps (the final two LL gaps that are not in the mixed regime) are approximately field independent and diverge from the cyclotron energy scale. This is best illustrated by plotting the LL gaps within a fixed density range [Fig. 2(k)]. It is surprising that for any given hole density, multiple LL gaps are set by a scale comparable to, but smaller than, the cyclotron energy. Similar plateaus persist across all three samples which were fabricated independently and exfoliated from bulk WSe_2 crystals from different sources, as well as a fourth device of Bernal bilayer WSe_2 (Supplemental Material Secs. 2, 5, and 6 [25]). This consistency indicates intrinsic and generic behavior unrelated to disorder or details of dielectric screening.

The gap we measure is equivalent to the particle-hole excitation energy [30]. Mapping the field dependence of these gaps thus allows us to determine the spin character of charge (hole) excitations. To address how different excitations evolve in a field, we consider the effects of Coulomb interactions on the spin-split LLs in WSe_2, beyond the general effect of a density-dependent spin susceptibility. Using Hartree-Fock calculations with RPA-screened interactions which take into account the large LL mixing in this material, we study the charge gaps from the highest-energy filled spin-majority LL [identified by its orbital index N and spin as $(|\nu| - 1, \uparrow)$] to both the subsequent spin-majority $(|\nu|, \uparrow)$ and lowest-energy spin-minority $(1, \downarrow)$ LLs (Supplemental Material Secs. 7 and 8 [25]). The resulting gaps are plotted in Figs. 2(f)–2(j), with a

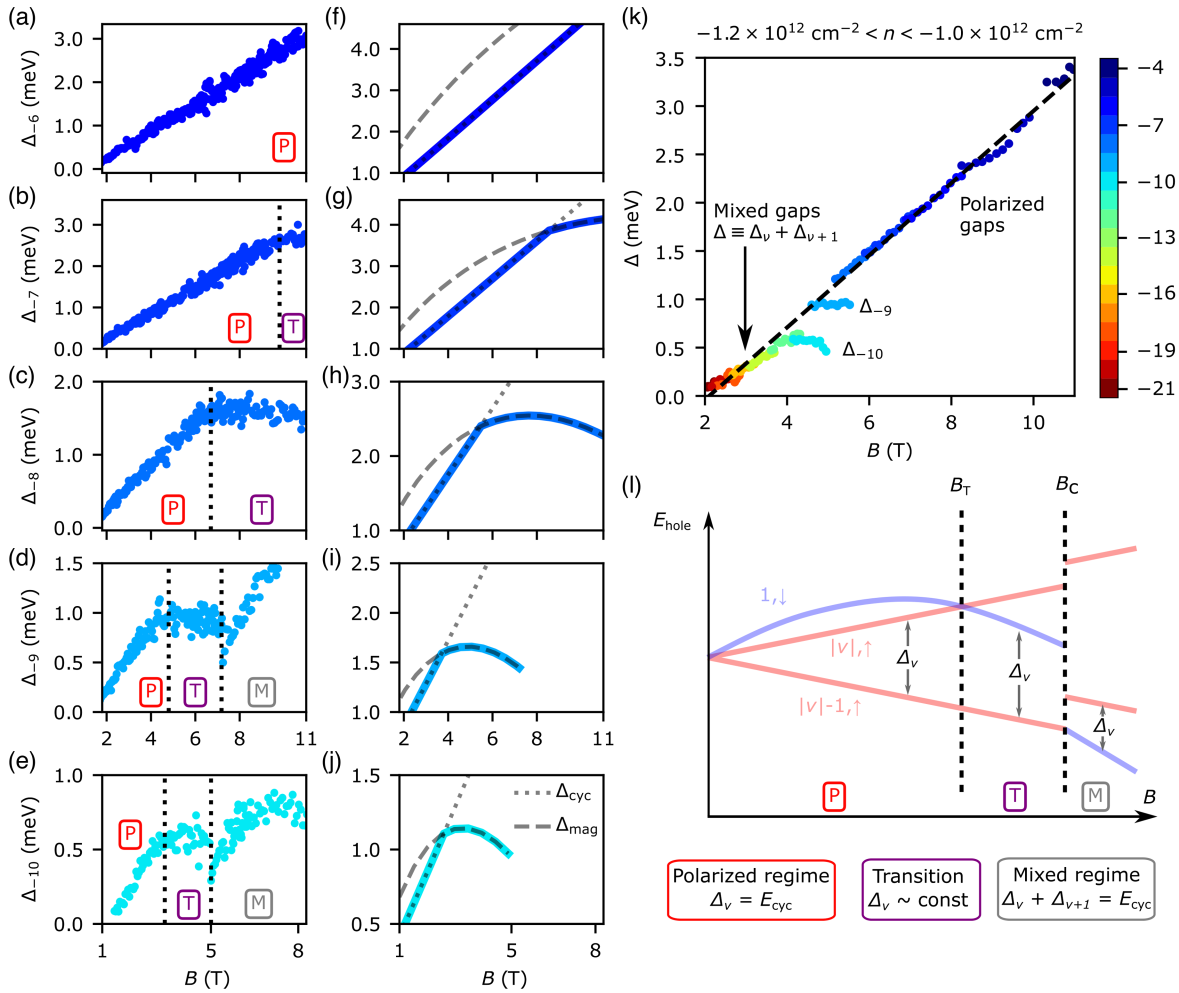

FIG. 2. Magnetic field dependence of LL gaps. (a)–(e) Experimentally measured LL gaps Δ_ν as a function of B for fixed integer values of the filling factor ν. We observe three distinct behaviors: fully polarized LLs with $\Delta_\nu = E_{cyc}$ (labeled by "P"), a transition region where Δ_ν plateaus (labeled by "T"), and a "mixed" regime where both spins are occupied and $\Delta_\nu + \Delta_{\nu+1} = E_{cyc}$ (labeled by "M"). Vertical dotted lines indicate boundaries separating these behaviors. (f)–(j) Corresponding theoretically predicted LL gaps from Hartree-Fock calculations with RPA-screened interactions. We show Δ_{cyc} (dotted lines), the gap to the next unoccupied majority spin LL, and Δ_{sf} (dashed lines), the gap to the $N = 1$ minority spin LL. The LL gap is the smaller of these (thick colored lines). (k) Measured gaps Δ as a function of B in the range $-1.2 \times 10^{12} < n < -1.0 \times 10^{12}$ cm^{-2}. Color indicates the filling factors of different gaps: Polarized and "transition" gaps (from $\nu = -4$ to $\nu = -10$) are plotted individually ($\Delta \equiv \Delta_\nu$), while the pairwise sum of gaps are plotted for even $\nu \leq -11$. The dashed black line is a linear fit (excluding the transition gaps). (l) Illustration of the LL energies relevant to Δ_ν, given in terms of $E_{hole} = -E$, so LLs are filled from the bottom up. At B_T, the lowest-energy LL above the gap switches from majority to minority spin, while at B_C, the system undergoes a first-order phase transition to the mixed regime.

schematic illustration of how the LL energies evolve with magnetic field in Fig. 2(l).

The gap to the next unoccupied spin-majority LL is mostly set by the cyclotron energy, as exchange interactions affect both majority-spin LLs similarly. The gap to the lowest spin-minority LL (the "spin-flip gap") is determined by both single-particle and exchange interactions; the latter strongly renormalize this gap because they have different effects on the particle and hole excitations. The relative balance of these two contributions at a given filling factor will vary as the magnetic field (and therefore carrier density) is tuned. At low magnetic fields, exchange interactions are comparatively stronger and disfavor minority spin occupation, increasing the spin-flip gap. At higher magnetic fields, the kinetic energy dominates the behavior, leading to a linear decrease with B from the large orbital mismatch between the relevant LLs. The result is a nonmonotonic dependence of the spin-flip gap with B so that it becomes competitive (and is eventually favored) compared with the cyclotron gap (Supplemental Material Sec. VIII [25]).

Our numerical calculations [Figs. 2(f)–2(j)] indicate that for the LLs we probe in our experiment, the curvature of the spin-flip gap is quite low at the crossover field B_T. This qualitatively matches the plateaus we observe over an intermediate field range in our measurements. We therefore interpret the transition region as a spin-polarized ground state that favors occupation of an opposite spin LL upon doping. At higher magnetic fields ($B > B_C$), the system undergoes a first-order transition to a mixed regime where the $(1, \downarrow)$ LL jumps to lower energy than the $(|\nu| - 1, \uparrow)$ state. The precise ordering of LLs [for example, whether the $(1, \downarrow)$ LL also jumps below the $(|\nu| - 2, \uparrow)$ state] is sensitive to details of the approximation in our theoretical calculations (Supplemental Material Sec. VIII [25]) and is ambiguous in experiment, so we restrict our quantitative comparison to $B < B_C$ in Fig. 2.

IV. REENTRANT MAGNETISM AND FULL SPIN PHASE DIAGRAM

The close competition between distinct phases also affects the behavior of the system at partial LL filling. Our measurements near each LL phase transition reveal a sharp negative compressibility feature emanating outward toward lower hole density as the field decreases [Figs. 3(a)–3(c)]. We interpret this behavior, indicative of a first-order isospin phase transition [31–34], as an extension of the LL reordering into compressible states of a partially filled LL [Fig. 3(d)].

As holes are initially depleted from integer filling [pink region, Fig. 3(d)], holes are removed from the highest-energy majority spin LL [Fig. 3(e)]. This depletion will decrease the exchange interactions, and the partially filed LL will be pushed toward the unoccupied minority spin LL. As additional holes are removed and the sample enters the gray region in Fig. 3(d), there is an abrupt reordering of spins and the minority spin LL is instead occupied [Fig. 3(f)]. Similar phenomenology was also suggested by recent transport measurements in a related system [24]. These transitions at partial LL filling, along with the observation of multiple LL gap plateaus at fixed n (varying B), imply reentrant spin polarization as the system sequentially fills, depletes, and again fills holes into the $N = 1$ minority spin LL. This leads to a "sawtooth" boundary between fully and partially spin-polarized phases in the n-B plane, which we show in the full spin phase diagram in Fig. 3(g).

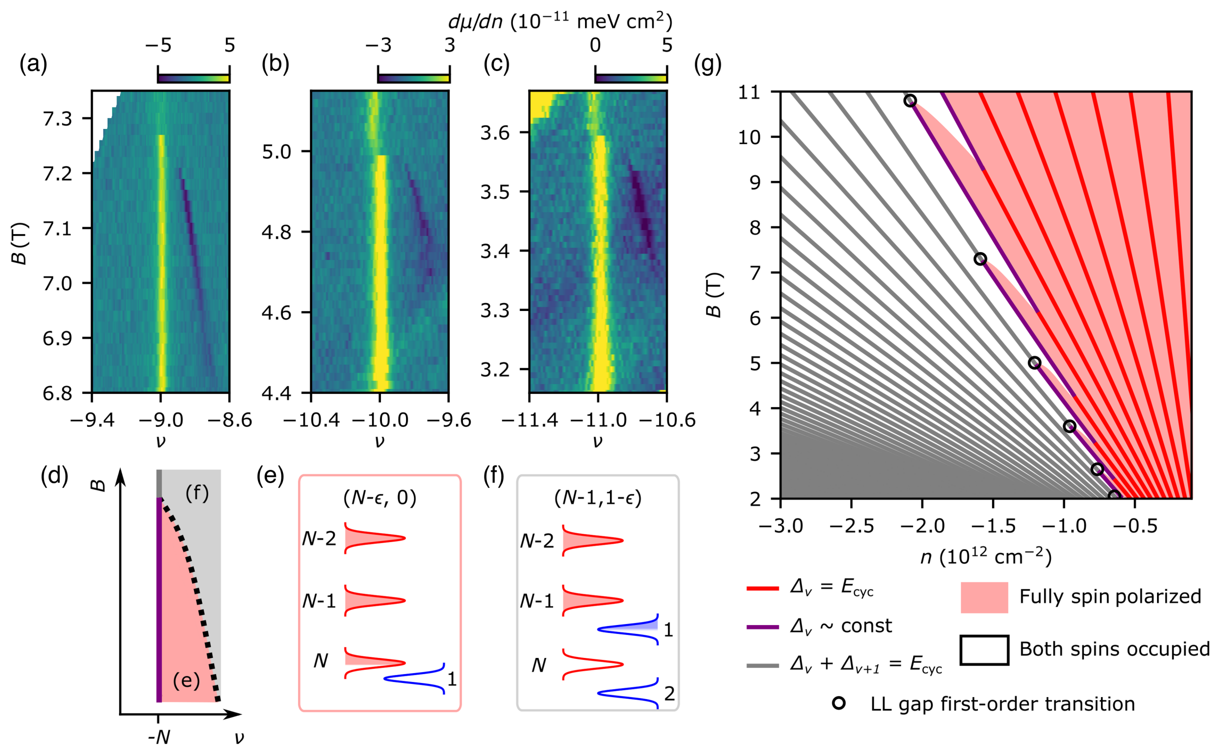

FIG. 3. Spin transitions within partially filled LLs and full phase diagram. (a)–(c) High-resolution measurements of $d\mu/dn$ near phase transitions at $\nu = -9, -10, -11$, highlighting the negative compressibility which extends into the adjacent LL. Panel (a) is measured at temperature $T = 1.6$ K, while panels (b) and (c) are at $T = 0.35$ K. The small shift in ν of the incompressible peak that occurs across the phase transition in (b) and (c) likely reflects asymmetry in the broadening of the crossing LLs (Supplemental Material Sec. X [25]). (d) Schematic showing regions of distinct partially occupied LLs as a function of B when $|\nu| \leq N$ for a given integer N. The pink shaded region corresponds to a fully polarized phase, with filling $(|\nu_\uparrow|, |\nu_\downarrow|) = (N - \epsilon, 0)$, where $\nu_{\uparrow(\downarrow)}$ is the filling factor of holes in the spin-$\uparrow$ (spin-$\downarrow$) sector and $0 < \epsilon < 1$. The light gray region is a mixed state with $(|\nu_\uparrow|, |\nu_\downarrow|) = (N - 1, 1 - \epsilon)$; i.e., a minority spin LL is partially filled. (e) and (f) Schematic of the LL orderings in each compressible phase, with red spin majority and blue spin minority LLs labeled by their respective orbital indices. (g) Schematic depiction of the full spin phase diagram as a function of n and B. Lines indicate the LL gap behavior, while shading indicates the spin character of the filled states.

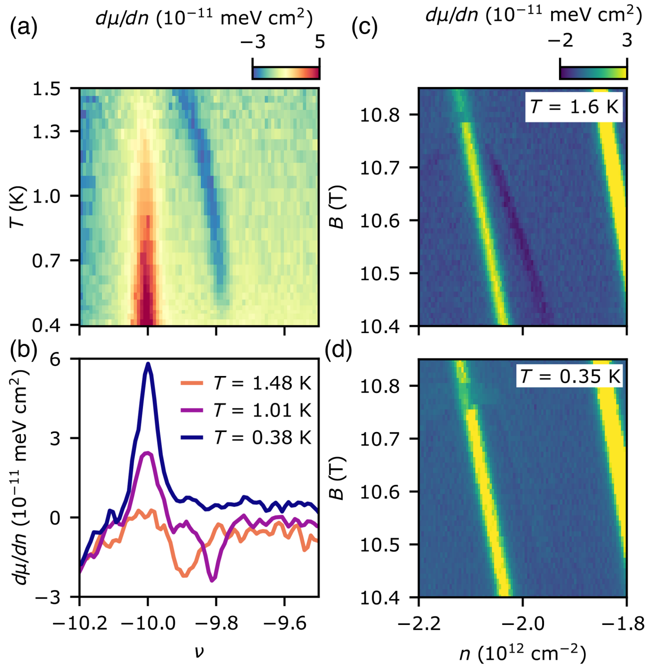

FIG. 4. Temperature dependence of the spin phase transition (a) $d\mu/dn$ as a function of T and ν at $B = 4.85$ T. As the temperature decreases, the LL gap becomes stronger and the negative compressibility moves farther away from integer filling and weakens at the lowest temperatures. (b) Line cuts of $d\mu/dn$ from panel (a) at select temperatures. (c) and (d) $d\mu/dn$ around the $\nu = -8$ transition at $T = 1.6$ K (c) and $T = 0.35$ K (d).

Finally, we discuss how these phase transitions depend on temperature, which provides further insight into the relative free energies of distinct states. In Figs. 4(a) and 4(b), we show $d\mu/dn$ as a function of ν and temperature T at a constant magnetic field $B = 4.85$ T [near the $\nu = -10$ transition shown in Fig. 3(b)]. The negative compressibility feature shifts to lower hole density as the system cools between $T = 1.5$ K and $T = 0.35$ K, indicating that the mixed phase is favored at higher temperatures and thus carries higher relative entropy.

The incompressible LL gap significantly strengthens at lower temperatures, as expected. In contrast, the negative compressibility weakens at the lowest temperatures of our measurement, displaying a nonmonotonic magnitude as a function of temperature. This contrasts with measurements of isospin transitions in distinct systems, where such features sharpen at lower temperatures [32–36]. In Figs. 4(c) and 4(d), we compare $d\mu/dn$ around the $\nu = -8$ transition at $T = 1.6$ K and $T = 0.35$ K, demonstrating that negative compressibility is barely visible at the lowest temperatures of our measurement. To explain this behavior, we use a Sommerfeld expansion to obtain a phenomenological model for the free energy around the phase transition. We find that at sufficiently low T, the relative slopes of the free energy as a function of density will be closer together due to an asymmetry in the density of states of the two phases, suppressing the negative $d\mu/dn$ at the phase transition (Supplemental Material Sec. X [25]).

V. OUTLOOK

In conclusion, our experiments reveal singular changes in the interaction-induced renormalization of LL energies at the crossover between spin-polarized and mixed states. The intertwined electronic and magnetic structure in this system enables gate control over macroscopic changes in magnetization at the Fermi level. Our results are relevant to a wider class of systems where many-body effects are even more prominent. While the sizable single-particle Zeeman energies characteristic of monolayer WSe_2 make the system susceptible to spin polarization even without interactions, related systems have displayed exchange driven polarization in the absence of a large Zeeman energy [37,38]. Interaction-induced polarization (and related phase transitions) is also relevant within moiré heterostructures, in which flat moiré bands quench the kinetic energy akin to LLs and complete spin polarization can be favored at both zero and finite magnetic field [34,35,39–41]. Our comprehensive understanding of the relative kinetic and interaction effects at transitions between full and partial spin polarization provides a framework for both experimental and theoretical study of energetics within these still more strongly interacting platforms.

ACKNOWLEDGMENTS

We acknowledge helpful conversations with Allan H. MacDonald and Brian Skinner. Device fabrication and scanning single-electron transistor measurements were primarily supported by NSF-DMR-2103910. Supporting data from bilayer WSe_2 was supported by the U.S. Department of Energy, Office of Basic Energy Sciences, Award No. DE-SC0023109. V. C., Z. H., and S. A. K. were supported by U.S. Department of Energy, Office of Basic Energy Sciences, under Contract No. DE-AC02-76SF00515. Synthesis of WSe_2 (S. L., J. H.) was supported by NSF MRSEC program at Columbia through the Center for Precision-Assembled Quantum Materials (DMR-2011738). K. W. and T. T. acknowledge support from the JSPS KAKENHI (Grants No. 20H00354 and No. 23H02052) and World Premier International Research Center Initiative (WPI), MEXT, Japan. B. A. F. acknowledges support from a Stanford Graduate Fellowship. Part of this work was performed at the Stanford Nano Shared Facilities (SNSF), supported by the National Science Foundation under Award No. ECCS-2026822.

[1] S. L. Sondhi, A. Karlhede, S. A. Kivelson, and E. H. Rezayi, *Skyrmions and the crossover from the integer to fractional quantum Hall effect at small Zeeman energies*, Phys. Rev. B **47**, 16419 (1993).

[2] V. Piazza, V. Pellegrini, F. Beltram, W. Wegscheider, T. Jungwirth, and A. H. MacDonald, *First-order phase transitions in a quantum Hall ferromagnet*, Nature (London) **402**, 638 (1999).

[3] E. Tutuc, E. P. De Poortere, S. J. Papadakis, and M. Shayegan, *In-plane magnetic field-induced spin polarization and transition to insulating behavior in two-dimensional hole systems*, Phys. Rev. Lett. **86**, 2858 (2001).

[4] O. Gunawan, Y. P. Shkolnikov, K. Vakili, T. Gokmen, E. P. De Poortere, and M. Shayegan, *Valley susceptibility of an interacting two-dimensional electron system*, Phys. Rev. Lett. **97**, 186404 (2006).

[5] K. Nomura and A. H. MacDonald, *Quantum Hall ferromagnetism in graphene*, Phys. Rev. Lett. **96**, 256602 (2006).

[6] T. M. Kott, B. Hu, S. H. Brown, and B. E. Kane, *Valley-degenerate two-dimensional electrons in the lowest Landau level*, Phys. Rev. B **89**, 041107(R) (2014).

[7] B. M. Hunt *et al.*, *Direct measurement of discrete valley and orbital quantum numbers in bilayer graphene*, Nat. Commun. **8**, 948 (2017).

[8] Q. Shi *et al.*, *Bilayer* $\mathrm{WSe_2}$ *as a natural platform for interlayer exciton condensates in the strong coupling limit*, Nat. Nanotechnol. **17**, 577 (2022).

[9] Q. Shi, E.-M. Shih, M. V. Gustafsson, D. A. Rhodes, B. Kim, K. Watanabe, T. Taniguchi, Z. Papić, J. Hone, and C. R. Dean, *Odd- and even-denominator fractional quantum Hall states in monolayer* $\mathrm{WSe_2}$, Nat. Nanotechnol. **15**, 569 (2020).

[10] D. Maryenko, J. Falson, Y. Kozuka, A. Tsukazaki, and M. Kawasaki, *Polarization-dependent Landau level crossing in a two-dimensional electron system in a* MgZnO/ZnO *heterostructure*, Phys. Rev. B **90**, 245303 (2014).

[11] J. Falson and M. Kawasaki, *A review of the quantum Hall effects in MgZnO/ZnO heterostructures*, Rep. Prog. Phys. **81**, 056501 (2018).

[12] F. F. Fang and P. J. Stiles, *Effects of a tilted magnetic field on a two-dimensional electron gas*, Phys. Rev. **174**, 823 (1968).

[13] J. Zhu, H. L. Stormer, L. N. Pfeiffer, K. W. Baldwin, and K. W. West, *Spin susceptibility of an ultra-low-density two-dimensional electron system*, Phys. Rev. Lett. **90**, 056805 (2003).

[14] R. J. Nicholas, R. J. Haug, K. v. Klitzing, and G. Weimann, *Exchange enhancement of the spin splitting in a* $\mathrm{GaAs-Ga_xAl_{1-x}As}$ *heterojunction*, Phys. Rev. B **37**, 1294 (1988).

[15] S. E. Barrett, G. Dabbagh, L. N. Pfeiffer, K. W. West, and R. Tycko, *Optically pumped NMR evidence for finite-size skyrmions in GaAs quantum wells near Landau level filling* $\nu = 1$, Phys. Rev. Lett. **74**, 5112 (1995).

[16] E. Tutuc, S. Melinte, and M. Shayegan, *Spin polarization and g factor of a dilute GaAs two-dimensional electron system*, Phys. Rev. Lett. **88**, 036805 (2002).

[17] X. Xu, W. Yao, D. Xiao, and T. F. Heinz, *Spin and pseudospins in layered transition metal dichalcogenides*, Nat. Phys. **10**, 343 (2014).

[18] M. V. Gustafsson, M. Yankowitz, C. Forsythe, D. Rhodes, K. Watanabe, T. Taniguchi, J. Hone, X. Zhu, and C. R. Dean, *Ambipolar Landau levels and strong band-selective carrier interactions in monolayer* $\mathrm{WSe_2}$, Nat. Mater. **17**, 411 (2018).

[19] Z. Wang, J. Shan, and K. F. Mak, *Valley- and spin-polarized Landau levels in monolayer* $\mathrm{WSe_2}$, Nat. Nanotechnol. **12**, 144 (2017).

[20] H. C. P. Movva, B. Fallahazad, K. Kim, S. Larentis, T. Taniguchi, K. Watanabe, S. K. Banerjee, and E. Tutuc, *Density-dependent quantum Hall states and Zeeman splitting in monolayer and bilayer* $\mathrm{WSe_2}$, Phys. Rev. Lett. **118**, 247701 (2017).

[21] S. Larentis, H. C. P. Movva, B. Fallahazad, K. Kim, A. Behroozi, T. Taniguchi, K. Watanabe, S. K. Banerjee, and E. Tutuc, *Large effective mass and interaction-enhanced Zeeman splitting of K-valley electrons in* $\mathrm{MoSe_2}$, Phys. Rev. B **97**, 201407(R) (2018).

[22] R. Pisoni *et al.*, *Interactions and magnetotransport through spin-valley coupled Landau levels in monolayer* $\mathrm{MoS_2}$, Phys. Rev. Lett. **121**, 247701 (2018).

[23] J. Li, M. Goryca, N. P. Wilson, A. V. Stier, X. Xu, and S. A. Crooker, *Spontaneous valley polarization of interacting carriers in a monolayer semiconductor*, Phys. Rev. Lett. **125**, 147602 (2020).

[24] E.-M. Shih *et al.*, *Spin-selective magneto-conductivity in* $\mathrm{WSe_2}$, arXiv:2307.00446.

[25] See Supplemental Material at http://link.aps.org/supplemental/10.1103/PhysRevX.14.031018 for supporting experimental data and details of theoretical modeling.

[26] J. Pack *et al.*, *Charge-transfer contact to a high-mobility monolayer semiconductor*, arXiv:2310.19782.

[27] K. Vakili, Y. P. Shkolnikov, E. Tutuc, E. P. De Poortere, and M. Shayegan, *Spin susceptibility of two-dimensional electrons in narrow AlAs quantum wells*, Phys. Rev. Lett. **92**, 226401 (2004).

[28] C. Attaccalite, S. Moroni, P. Gori-Giorgi, and G. B. Bachelet, *Correlation energy and spin polarization in the 2D electron gas*, Phys. Rev. Lett. **88**, 256601 (2002).

[29] T. Ando and Y. Uemura, *Theory of quantum transport in a two-dimensional electron system under magnetic fields. I. Characteristics of level broadening and transport under strong fields*, J. Phys. Soc. Jpn. **36**, 959 (1974).

[30] B. A. Foutty, J. Yu, T. Devakul, C. R. Kometter, Y. Zhang, K. Watanabe, T. Taniguchi, L. Fu, and B. E. Feldman, *Tunable spin and valley excitations of correlated insulators in* Γ*-valley moiré bands*, Nat. Mater. **22**, 731 (2023).

[31] J. P. Eisenstein, L. N. Pfeiffer, and K. W. West, *Negative compressibility of interacting two-dimensional electron and quasiparticle gases*, Phys. Rev. Lett. **68**, 674 (1992).

[32] B. E. Feldman, A. J. Levin, B. Krauss, D. A. Abanin, B. I. Halperin, J. H. Smet, and A. Yacoby, *Fractional quantum Hall phase transitions and four-flux states in graphene*, Phys. Rev. Lett. **111**, 076802 (2013).

[33] H. Zhou *et al.*, *Half- and quarter-metals in rhombohedral trilayer graphene*, Nature (London) **598**, 429 (2021).

[34] J. Yu *et al.*, *Correlated Hofstadter spectrum and flavour phase diagram in magic-angle twisted bilayer graphene*, Nat. Phys. **18**, 825 (2022).

[35] C. R. Kometter, J. Yu, T. Devakul, A. P. Reddy, Y. Zhang, B. A. Foutty, K. Watanabe, T. Taniguchi, L. Fu, and B. E. Feldman, *Hofstadter states and re-entrant charge order in a semiconductor moiré lattice*, Nat. Phys. **19**, 1861 (2023).

[36] B. A. Foutty, C. R. Kometter, T. Devakul, A. P. Reddy, K. Watanabe, T. Taniguchi, L. Fu, and B. E. Feldman, *Mapping twist-tuned multiband topology in bilayer* WSe_2, Science **384**, 343 (2024).
[37] J. G. Roch, G. Froehlicher, N. Leisgang, P. Makk, K. Watanabe, T. Taniguchi, and R. J. Warburton, *Spin-polarized electrons in monolayer* MoS_2, Nat. Nanotechnol. **14**, 432 (2019).
[38] N. Leisgang *et al.*, *Exchange energy of the ferromagnetic electronic ground-state in a monolayer semiconductor* Phys. Rev. Lett. **133**, 026501 (2024).
[39] U. Zondiner *et al.*, *Cascade of phase transitions and Dirac revivals in magic-angle graphene*, Nature (London) **582**, 203 (2020).
[40] Y. Saito, F. Yang, J. Ge, X. Liu, T. Taniguchi, K. Watanabe, J. I. A. Li, E. Berg, and A. F. Young, *Isospin Pomeranchuk effect in twisted bilayer graphene*, Nature (London) **592**, 220 (2021).
[41] E. Anderson, F.-R. Fan, J. Cai, W. Holtzmann, T. Taniguchi, K. Watanabe, D. Xiao, W. Yao, and X. Xu, *Programming correlated magnetic states with gate-controlled moiré geometry*, Science **381**, 325 (2023).